

• 水利工程 •

DOI:10.12454/j.jsuese.202300564



本刊网刊

采砂活动对三峡坝下游沙质河段泥沙冲淤影响研究

陈柄君, 肖毅

(重庆交通大学 国家内河航道整治工程技术研究中心, 重庆 400074)

摘要:以三峡工程为核心的梯级水库群联合调度运用改变了坝下游水沙条件,引起长时间、长距离的冲淤调整,尤其是近坝段沙质河床调整显著。长江沿线经济建设的飞速发展促进了对长江流域江砂资源的需求,坝下游采砂活动使得近坝段河床冲淤、洲滩调整过程更为复杂。为探究采砂对坝下游沙质河段泥沙冲淤特性的影响,以坝下游沙市河段为例,基于Delft3D建立了平面2维水沙数值模型,模拟了采砂活动影响下河段泥沙冲淤变化过程,分析了采砂前后河段冲淤分布、含沙量分布、冲淤量变化等。结果表明:河槽内百万 m^3 量级采砂坑对其上下游约1 km范围内泥沙冲淤变幅略有影响,幅度为 $-0.1\sim 0.1$ m;对整个河段冲淤特性影响较小,采砂前后河段整体冲淤量变化约为6%;采砂坑恢复能力与该河段来水来沙关系密切,正常水文年的年均回淤率为10%~25%,而在异常水文年(大水大沙)的年均回淤率可达50%,其恢复周期约为4~10 a。

关键词:沙市河段;采砂活动;泥沙冲淤;采砂坑恢复能力;三峡大坝坝下游河段

中图分类号:TV147.3

文献标志码:A

文章编号:2096-3246(2025)03-0201-09

近年来,随着以三峡工程为核心的长江上游水库群逐步建成并联合调度运用,特别是金沙江下游溪洛渡、向家坝水库建成后,坝下游河道水沙条件^[1-2]、河床演变过程及趋势^[3-5]都发生了深刻的改变。自2003年三峡水库蓄水运行后,坝下游沙市河段总体呈现冲刷态势^[6],滩槽格局和洲滩变化显著^[7-8],汉道主流摆动较大^[9-10],处于强烈河床调整过程。

长江河道砂源丰富,河砂采挖、运移会改变局部水动力条件,破坏原有河道冲淤平衡状态^[11]。2016年以前,长江中下游的采砂活动剧烈,疏浚抛沙、河道采砂等人类活动一定程度上改变了局部河床的冲淤强度,过量无序采砂引起河段局部水位下降、洲滩稳定性减弱,从而给河道河势稳定及通航条件带来不利影响^[12-14]。目前,采砂活动对河段冲淤特性影响方面的研究主要采用物理模型与数学模型两种方法。物理模型^[15]能通过概化试验明确采砂坑对小尺度河床地形改变的影响,但在长河段长时段影响机制研究方面

存在成本高与比尺效应复杂等问题,因此不少学者通过建立水沙数学模型探究采砂活动对河段冲淤^[16-19]、河床演变^[20-23]及通航条件^[24-25]的影响作用,但对于采砂坑自身恢复期的研究仍较少。

本文以三峡坝下游沙市河段为研究对象,利用2019—2021年沙市二郎矶水文站实测水沙资料及2018年12月实测地形资料,基于Delft3D建立平面2维水沙数值模型,模拟采砂前后河段冲淤分布、冲淤量变化、含沙量等特征参量变化,分析采砂活动对河段冲淤变化的影响,研究不同水文年下的采砂坑恢复能力(回淤率、回淤周期等)。

1 Delft3D模型概述

本文采用Delft3D的2D-FLOW与SED模块。2D-FLOW基于正交曲线坐标和球面坐标系,采用的2维浅水方程为由不可压缩流体N-S方程简化的沿 ξ 、 η 方向动量方程,基本控制方程如下:

收稿日期:2023-07-25 修回日期:2023-10-24 网络出版日期:2024-01-25

基金项目:国家自然科学基金项目(52179059);重庆市自然科学基金项目(cstc2021jcyj-msxmX0490)

作者简介:陈柄君(1998—),男,硕士生.研究方向:航道整治. E-mail:cbj19981029@163.com

*通信作者:肖毅,教授, E-mail:xytmlove@163.com

$$\frac{\partial \zeta}{\partial t} + \frac{1}{\sqrt{G_{\zeta\zeta}} \sqrt{G_{\eta\eta}}} \cdot \left(\frac{\partial [(d+\zeta)U \sqrt{G_{\eta\eta}}]}{\partial \zeta} + \frac{\partial [(d+\zeta)V \sqrt{G_{\zeta\zeta}}]}{\partial \eta} \right) = Q \quad (1)$$

$$\begin{aligned} \frac{\partial u}{\partial t} + \frac{u}{\sqrt{G_{\zeta\zeta}}} \cdot \frac{\partial u}{\partial \zeta} + \frac{u}{\sqrt{G_{\eta\eta}}} \cdot \frac{\partial u}{\partial \eta} + \frac{\omega}{d+\zeta} \cdot \frac{\partial u}{\partial \sigma} + \\ \frac{uv}{\sqrt{G_{\zeta\zeta}} \sqrt{G_{\eta\eta}}} \cdot \frac{\partial \sqrt{G_{\eta\eta}}}{\partial \eta} - \frac{v\eta}{\sqrt{G_{\zeta\zeta}} \sqrt{G_{\eta\eta}}} \cdot \frac{\partial \sqrt{G_{\eta\eta}}}{\partial \eta} - \\ f\eta = -\frac{1}{\rho_0 \sqrt{G_{\zeta\zeta}}} P_\zeta + F_\zeta + \frac{1}{(d+\zeta)^2} \cdot \frac{\partial}{\partial \sigma} \left(v_v \frac{\partial u}{\partial \sigma} \right) + M_\zeta \end{aligned} \quad (2)$$

$$\begin{aligned} \frac{\partial v}{\partial t} + \frac{u}{\sqrt{G_{\zeta\zeta}}} \cdot \frac{\partial v}{\partial \zeta} + \frac{v}{\sqrt{G_{\eta\eta}}} \cdot \frac{\partial v}{\partial \eta} + \frac{\omega}{d+\zeta} \cdot \frac{\partial v}{\partial \sigma} + \\ \frac{uv}{\sqrt{G_{\zeta\zeta}} \sqrt{G_{\eta\eta}}} \cdot \frac{\partial \sqrt{G_{\eta\eta}}}{\partial \zeta} - \frac{uu}{\sqrt{G_{\zeta\zeta}} \sqrt{G_{\eta\eta}}} \cdot \frac{\partial \sqrt{G_{\zeta\zeta}}}{\partial \eta} - \\ f\eta = -\frac{1}{\rho_0 \sqrt{G_{\eta\eta}}} P_\eta + F_\eta + \frac{1}{(d+\zeta)^2} \cdot \frac{\partial}{\partial \sigma} \left(v_v \frac{\partial v}{\partial \sigma} \right) + M_\eta \end{aligned} \quad (3)$$

式(1)~(3)中, d 为相对于参考平面的水深, f 为科氏力系数, ζ 为相对于参考平面的水位, $\sqrt{G_{\zeta\zeta}}$ 为 ζ 方向上的坐标转换系数, U 为 ζ 方向上的平均速度, $\sqrt{G_{\eta\eta}}$ 为 η 方向上的坐标转换系数, V 为 η 方向上的平均速度, Q 为单位面积水量变化值, P_ζ 和 P_η 分别代表 ζ 和 η 方向的压力梯度, F_ζ 和 F_η 分别代表 ζ 和 η 方向的不平衡的水平应力, M_ζ 和 M_η 代表源项和汇项带来的外部动量, u 、 v 、 ω 分别为 ζ 、 η 、 σ 方向上的速度值, t 为时间, ρ_0 为水体密度, v_v 为垂向紊动系数。

Delft3D的SED模块可用于模拟黏性、非黏性沙平衡或非平衡输移过程,本文采用的泥沙输移控制方程为:

$$\begin{aligned} \frac{\partial (hc_i)}{\partial t} + \frac{1}{\sqrt{G_{\zeta\zeta}} \sqrt{G_{\eta\eta}}} \cdot \left[\frac{\partial (\sqrt{G_{\eta\eta}} h \bar{u} c_i)}{\partial \zeta} + \frac{\partial (\sqrt{G_{\zeta\zeta}} h \bar{v} c_i)}{\partial \eta} \right] - \\ \frac{1}{\sqrt{G_{\zeta\zeta}} \sqrt{G_{\eta\eta}}} \left[\frac{\partial}{\partial \zeta} \left(\sqrt{G_{\zeta\zeta}} \varepsilon_\zeta \frac{\partial hc_i}{\partial \zeta} \right) + \right. \\ \left. \frac{\partial}{\partial \eta} \left(\sqrt{G_{\eta\eta}} \varepsilon_\eta \frac{\partial hc_i}{\partial \eta} \right) \right] = S_i \end{aligned} \quad (4)$$

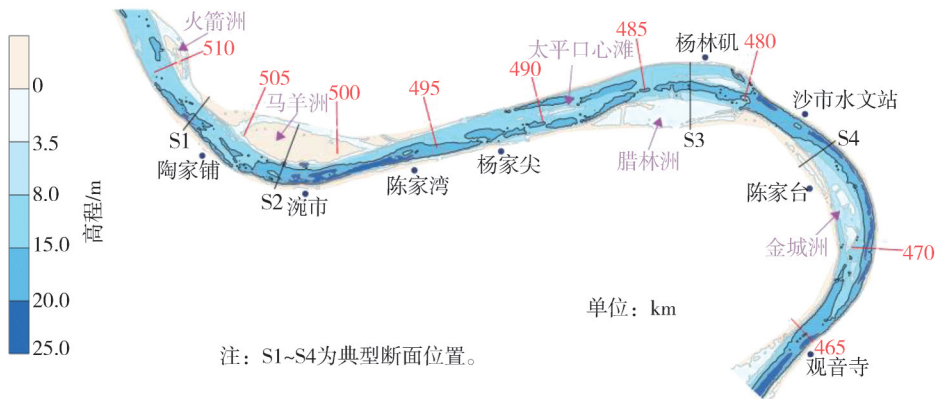
$$|S_{b,i}| = 0.006 \omega_{s,i} D_{50,i} \frac{u_{\text{eff}} (u_{\text{eff}} - u_{\text{cr},i})^{1.4}}{[(s_i - 1) g D_{50,i}]^{1.2}} \quad (5)$$

式(4)~(5)中, h 为水深, \bar{u} 为沿 ζ 方向的垂向平均流速, \bar{v} 为沿 η 方向的垂向平均流速, c_i 为第 i 组泥沙组分的浓度, ε_ζ 、 ε_η 为沿 ζ 、 η 方向的泥沙扩散系数, S_i 为第 i 组泥沙组分的源汇项, $|S_{b,i}|$ 为第 i 组非黏性组分的底沙单宽输运强度, u_{eff} 为垂向平均流速和近底波轨流速的合速度, $\omega_{s,i}$ 为第 i 个非黏性组分的沉降速度, $D_{50,i}$ 为第 i 个非黏性组分的中值粒径, $u_{\text{cr},i}$ 为基于希尔兹曲线得到的第 i 组非黏性组分临界起动速度。

2 沙市河段水沙模型构建

2.1 计算网格划分与条件选取

沙市河段位于上荆江中上段,航道里程510~465 km,全长约45 km,河道内滩群密布,自上而下分布着太平口心滩、腊林洲边滩、金城洲等,如图1所示。模型采用正交贴体曲线网格,网格划分如图2所示,网格数量为156×27,其中, M 向的网格长度为60~100 m, N 向的网格长度为20~40 m。



注: S1~S4为典型断面位置。

图1 沙市河段河势

Fig. 1 River pattern of the Shashi River section

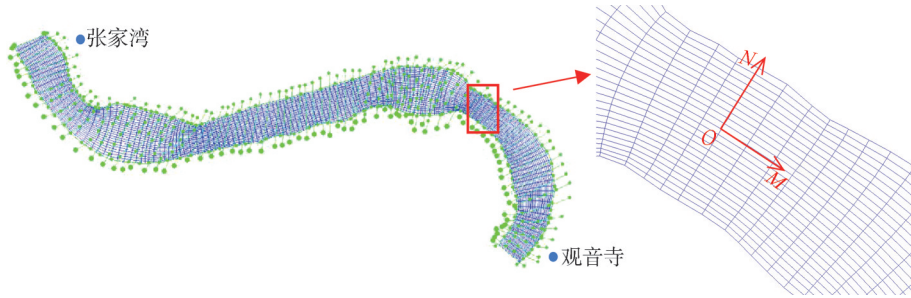


图2 模型网格划分

Fig. 2 Model grid partitioning

模型采用的初始计算地形为2018年8月1:10 000实测地形,进出口边界条件均采用沙市二郎矶水文站2019—2021年水沙实测资料^[26],水流计算步长为24 s,泥沙模块中值粒径为250 μm,河床活动层厚度为10 m,

泥沙模块计算时间步长为24 s。

2.2 沿程水位验证

图3为沙市河段2021年9、4和2月(洪、中、枯水期)的模拟与实测水位值对比分析结果。

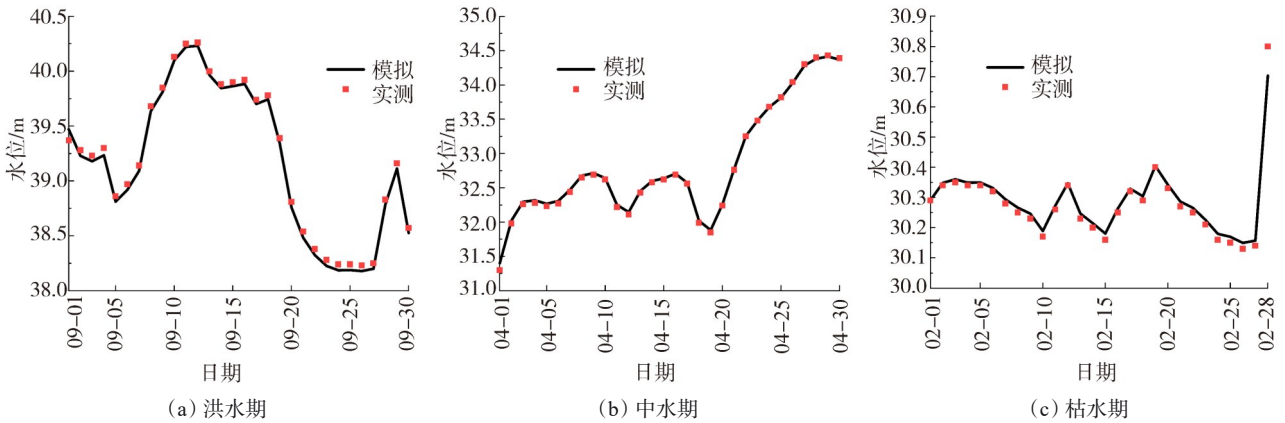


图3 沙市站不同水文条件下水位模拟与实测值对比

Fig. 3 Comparison of simulated and measured water level values at Shashi station under different hydrological conditions

由图3可知,所构建的2维水沙模型的计算水位与实测水位吻合良好,水位模拟均方根误差为0.92,其中,最大水位误差出现在2月28日,为0.08 m。总体而言,模型能较好模拟该河段水位变化过程。

由于岸线崩塌引起轻微淤积;陈家湾至杨林矶以冲刷为主,杨家尖附近轻微淤积;陈家台上游显著冲刷,最大冲深约6 m,金城洲中部显著淤积,主河槽内冲淤幅度为-5~3 m。

2.3 河道冲淤分布验证

表1为沙市河段2019—2021年模拟与实测的泥沙冲淤量对比,该河段主要表现为冲刷态势,实测与计算冲刷量相对误差为12%。图4为沙市河段模拟与实测冲淤分布。由图4可知:计算与实测冲淤分布基本保持一致,火箭洲、马羊洲左右汉以冲刷为主,岸边

表1 沙市河段泥沙实测与计算冲刷量

Tab. 1 Measurement and computation of sediment transport in the Shashi River section

河段长度/km	计算冲淤量/ (10 ⁴ m ³)	实测冲淤量/ (10 ⁴ m ³)	相对误差/%
45	-3 945	-3 513	12

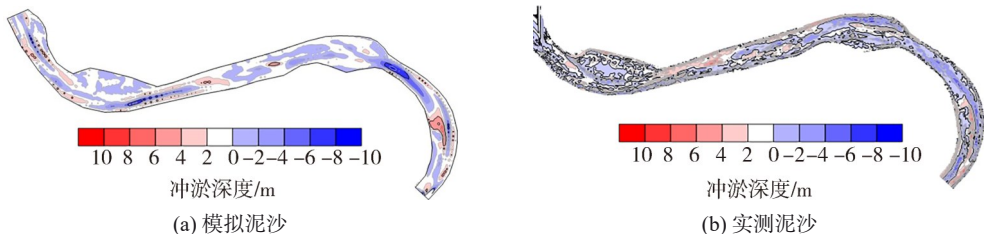


图4 沙市河段模拟与实测泥沙冲淤变化平面分布

Fig. 4 Calculated and measured erosion and deposition distribution in Shashi River section

图5为沙市河段典型断面实测与模拟地形变化对比。由图5可知:火箭洲至马羊洲的断面1冲淤变化

不大,断面形态较为稳定;横跨马羊洲的断面2左汉为微淤,淤积幅度为0.5 m,右汉则表现为微冲,冲刷幅度

约 1.5 m; 腊林洲附近断面 3 局部差别较大, 主要是由太平口水道 2021 年进行了约 $147.66 \times 10^4 \text{ m}^3$ 的航道疏浚所致; 沙市站下游断面 4 形态基本稳定, 最大冲深约 5 m。整体而言, 除局部有明显差别外, 典型断面计算与实测地形变化趋势基本一致, 模型能用于后续定量分析采砂活动对河段冲淤特性影响研究。

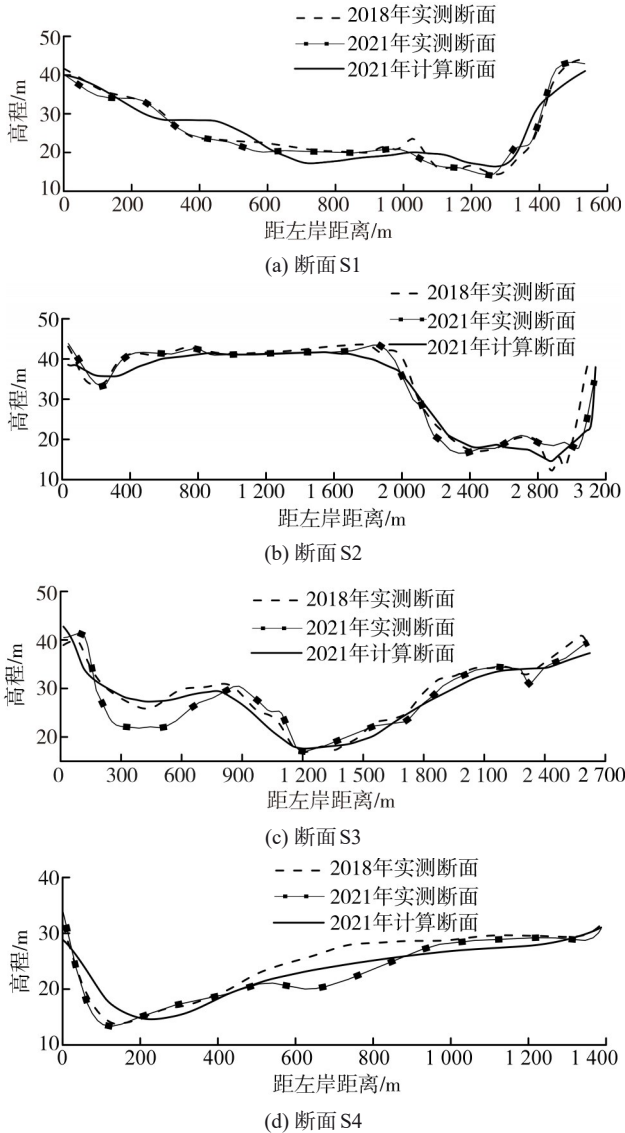
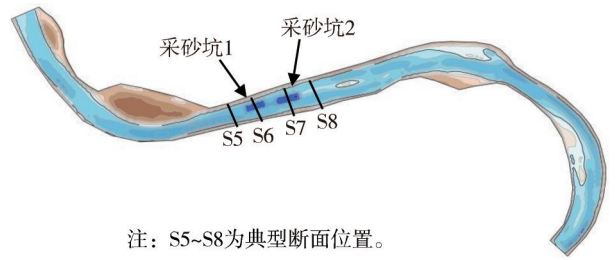


图 5 沙市河段计算与实测断面地形变化对比
Fig. 5 Comparison of calculated and measured changes in cross-sections in the Shashi River section

3 采砂活动对沙市河段冲淤特性影响

3.1 沙市河段概化采砂坑设置

2018 年以前, 该河段采砂活动主要发生在太平口心滩附近^[27], 因此, 根据实测资料, 基于 2018 年实测河床地形, 设置了两个概化采砂坑如图 6 所示, 采砂坑尺寸见表 2。整个模拟过程, 进出口水沙条件及计算参数设置与验证工况一致。



注: S5~S8 为典型断面位置。

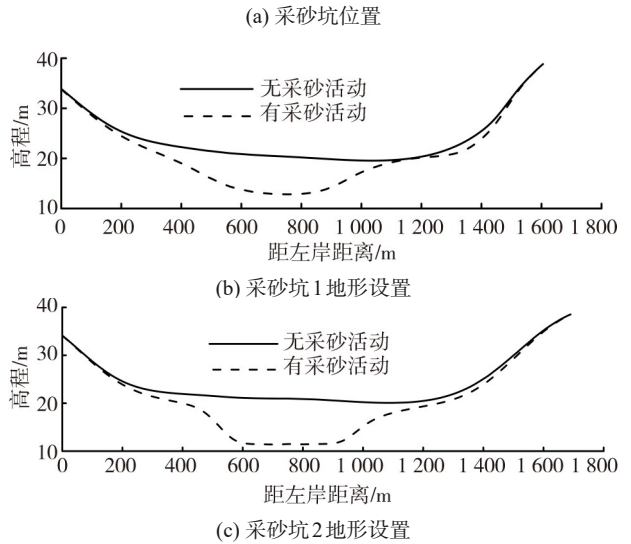


图 6 沙市河段概化采砂坑位置及采砂坑断面地形设置
Fig. 6 Layout of generalized sand mining pits and cross section configurations in the Shashi River section

表 2 沙市河段采砂坑设置参数

Tab. 2 Parameters for setting up a sand mining pit in the Shashi River section

采砂坑编号	长度/m	采砂坑平均深度/m	采砂坑体积/(10^4 m^3)
1	650	6.5	137
2	750	5.5	117

3.2 采砂对沙市河段泥沙输移过程影响

图 7 为 2020 年 3 月与 8 月采砂坑上、下游区域的含沙量变化。

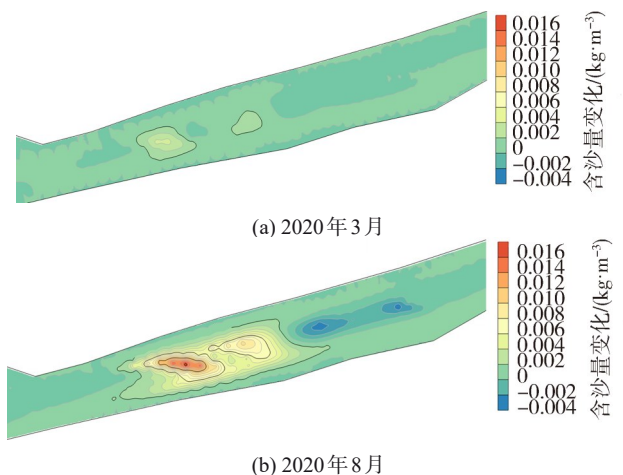


图 7 采砂坑上、下游含沙量变化
Fig. 7 Changes in the sediment concentration in the upstream and downstream of sand mining pits

由图7可知:采砂坑上、下游段整体含沙量变化受采砂影响不显著,变幅为 $0 \sim 0.002 \text{ kg/m}^3$,含沙量变化主要位于采砂坑。枯水期河段来水来沙均较小,含沙量变幅为 $0.004 \sim 0.006 \text{ kg/m}^3$;洪水期变幅增加,最大可达到 0.016 kg/m^3 。

表3为有无采砂情况下沙市河段计算冲淤量对比。由表3可知,该河段整体冲淤量受采砂影响不大,由于采砂坑回淤,有采砂坑条件下河段整体冲淤量略有降低,沙市河段整体冲淤变幅仅为 -5.7% 。

表3 沙市河段有无采砂工况下的计算冲淤量

Tab.3 Sedimentation volume in the Shashi River section with and without sand mining conditions

采砂情况	河段长度/km	冲淤量/(10^4 m^3)	相对变幅/%
有	45	-3 720	-5.7
无	45	-3 945	

图8为有无采砂影响的沙市河段冲淤分布。由图8可知:从泥沙冲淤分布来看,两种工况下河段主要冲淤部位基本一致,并未由于采砂活动引起河段的冲淤特性改变;而在经过2019、2020、2021这3个水文年后,采砂坑内显著回淤,最大淤积幅度约7 m,采砂坑上游冲刷强度略有加强,主要是由采砂坑上游近底流速增加引起底沙输移增加所致。

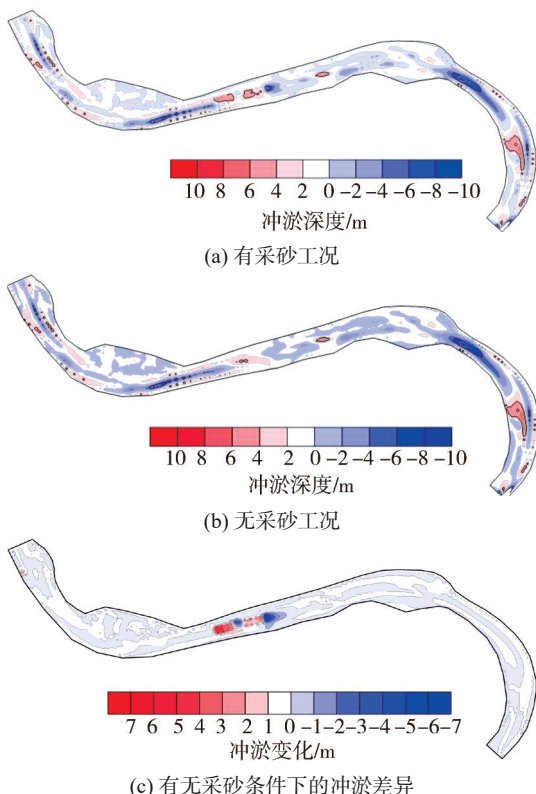


图8 沙市河段有无采砂工况下的冲淤分布
Fig.8 Distribution of erosion and deposition in the Shashi River section with and without sand mining

3.3 采砂坑恢复能力分析

图9为有无采砂条件的沙市河段典型断面地形变化对比。由图9可知:距采砂坑1上游300 m的典型断面S5在两种工况下地形变化一致;处于采砂坑1与采砂坑2区域的典型断面S6与S7则出现了快速淤积,最大淤积幅度约6.2 m;距采砂坑2下游500 m的断面S8在两种工况下地形变化基本一致。这说明独立采砂坑对下游河段整体冲淤影响较小。

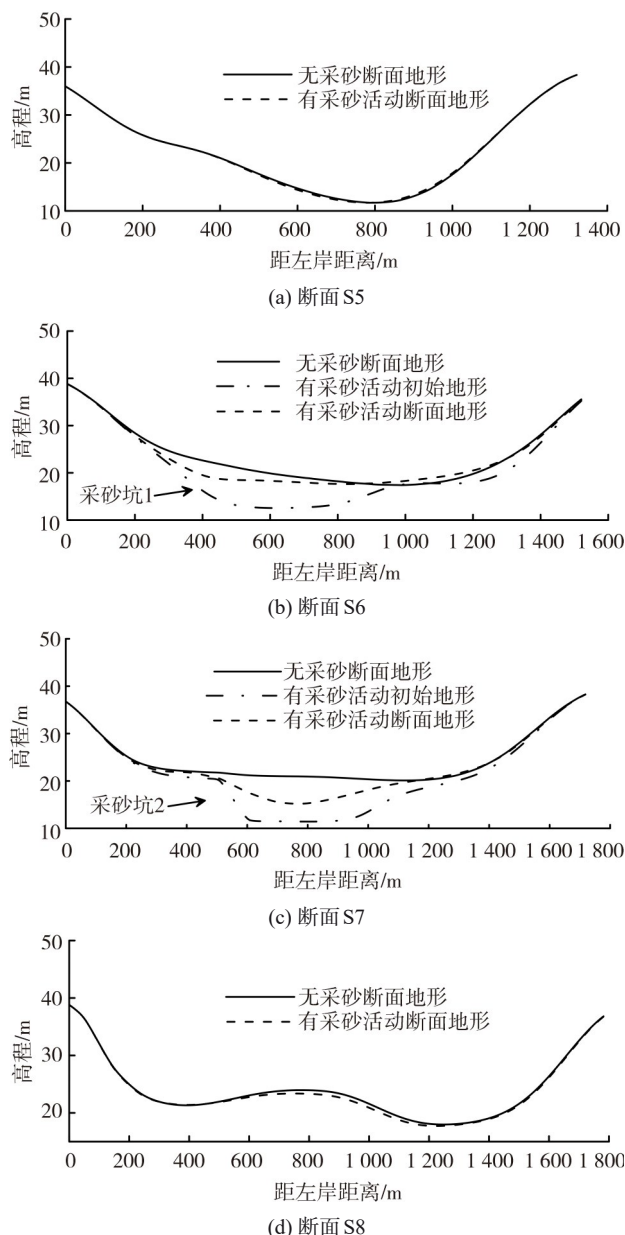


图9 沙市河段采砂坑附近典型断面地形变化
Fig.9 Changes in the typical cross-sectional topography of the Shashi River reach near the sand mining pits

表4统计了不同水文年下沙市河段概化采砂坑的年均回淤指标。表4中:2019年与2021年均均为正常水文年,输沙量约 $0.188 \times 10^8 \text{ t}$;2020年为大水大沙年,输沙

量达 0.587×10^8 t。由表 4 可知:在正常水文年(2019、2021 年),概化采砂坑的平均淤高为 0.9~1.3 m,年均回淤率约为 10%~25%;在异常水文年(2020 年),采砂坑各项回淤指标显著提高,年均淤高增至 3 m,回淤体积提升至 60×10^4 m³,回淤率增至约 50%。研究表明,沙市河段百万 m³ 量级采砂坑恢复能力与来水来沙条件密切相关,正常水文年下该河段采砂坑恢复周期约为 4~10 a,而大水大沙年会使恢复周期缩短。

表 4 采砂坑各水位年回淤统计参数

Tab. 4 Deposition parameters of sand mining pits in different hydrological year

采砂坑编号	年份	平均回淤厚度/m	回淤体积/ (10 ⁴ m ³)	回淤率/%
1	2019	0.9	18.95	13.80
	2020	3.1	65.29	47.65
	2021	1.3	27.38	19.98
2	2019	0.6	12.74	10.89
	2020	2.8	59.43	50.79
	2021	1.4	29.72	25.40

4 结 论

1) 基于 Delft3D 构建三峡坝下游沙市河段平面二维水沙数值模型,开展了 2019—2021 年河段泥沙冲淤过程模拟,计算冲淤分布与实测基本一致,冲淤量相对误差为 12%,表明构建的模型能较好地模拟沙市河段泥沙冲淤过程。

2) 开展了百万 m³ 量级采砂坑下河段泥沙冲淤变化计算,对比河道含沙量、冲淤量及冲淤分布表明,小规模河道采砂对河段整体泥沙输移过程影响较小,其含沙量变化影响范围小于 1 km,而变化显著体现在洪水期采砂坑区域,最大变幅可达 0.016 kg/m³,但河段整体冲淤特性并未改变。

3) 采砂坑恢复能力与河段来水来沙关系密切,正常水文年采砂坑年均回淤率约为 10%~25%,恢复周期约 10 a,而异常水文年(如大水大沙)的年均回淤率可达 50%。

参考文献:

[1] Zhang Wei, Wu Meiqin, Li Sixuan, et al. Mechanism of adjustment of scouring and silting of Chenglingji—Jiujiang reach in the middle reaches of the Yangtze River after impoundment of the Three Gorges Dam[J]. *Advances in Water Science*, 2020, 31(2): 162–171. [张为, 吴美琴, 李思璇, 等. 三峡水库蓄水后城陵矶至九江段河道冲淤调整机理[J]. *水科学进展*, 2020, 31(2): 162–171.]

[2] Wang Hualin, Zheng Shan, Tan Guangming, et al. Spatio-temporal channel evolution and the migration of erosion center in Yichang—Chenglingji Reach after the operation of the Three Gorges Project[J]. *Journal of Hydraulic Engineering*, 2021, 52(12): 1470–1481. [王华琳, 郑珊, 谈广鸣, 等. 三峡水库运行后宜昌—城陵矶河段冲刷重心下移与时空演变[J]. *水利学报*, 2021, 52(12): 1470–1481.]

[3] Li Ming, Hu Chunhong, Fang Chunming. Study on pattern and mechanism of river section topography adjustment in the downstream of the Three Gorges Project[J]. *Journal of Hydraulic Engineering*, 2018, 49(12): 1439–1450. [李明, 胡春宏, 方春明. 三峡水库坝下游河道断面形态调整模式与机理研究[J]. *水利学报*, 2018, 49(12): 1439–1450.]

[4] Han Jianqiao, Sun Zhaohua, Huang Ying, et al. Features and causes of sediment deposition and erosion in Jingjiang reach after impoundment of the Three Gorges Project[J]. *Journal of Hydraulic Engineering*, 2014, 45(3): 277–285. [韩剑桥, 孙昭华, 黄颖, 等. 三峡水库蓄水后荆江沙质河段冲淤分布特征及成因[J]. *水利学报*, 2014, 45(3): 277–285.]

[5] Mei Junya, Mao Beiping. A study on characteristics of water-sediment transport in Chenglingji—Wuhan Reach of the middle Changjiang River before and after the Three Gorges Reservoir impoundment[J]. *Journal of Basic Science and Engineering*, 2007(4): 473–482. [梅军亚, 毛北平. 三峡工程蓄水前后城陵矶至武汉河段水沙输移特性分析[J]. *应用基础与工程科学学报*, 2007(4): 473–482.]

[6] Fan Yongyang, Zhang Wei, Han Jianqiao, et al. The typical meandering river evolution adjustment and its driving mechanism in the downstream reach of TGR[J]. *Acta Geographica Sinica*, 2017, 72(3): 420–431. [樊咏阳, 张为, 韩剑桥, 等. 三峡水库下游弯曲河型演变规律调整及其驱动机制[J]. *地理学报*, 2017, 72(3): 420–431.]

[7] Yang Xuhai, Xiong Haibin, Li Yitian, et al. Adjustment mechanism of the typical sandbars in the lower Jingjiang River after the impoundment of the Three Gorges Reservoir[J]. *Journal of Lake Sciences*, 2021, 33(3): 819–829. [杨绪海, 熊海滨, 李义天, 等. 三峡水库蓄水后下荆江河段典型洲滩调整机理[J]. *湖泊科学*, 2021, 33(3): 819–829.]

[8] Xue Xinghua, Chang Sheng, Song Eping. Evolution of floodplains and bars at the Jingjiang reach of Yangtze River, China in response to Three Gorges Reservoir impoundment[J]. *Acta Geographica Sinica*, 2018, 73(9): 1714–1727. [薛兴华, 常胜, 宋鄂平. 三峡水库蓄水后荆江洲滩变化特征[J]. *地理学报*, 2018, 73(9): 1714–1727.]

[9] Xu Quanxi. Study of sediment deposition and erosion pat-

- terns in the middle and downstream Changjiang main-stream after impoundment of TGR[J]. *Journal of Hydroelectric Engineering*,2013,32(2):146–154.[许全喜.三峡工程蓄水运用前后长江中下游干流河道冲淤规律研究[J].水力发电学报,2013,32(2):146–154.]
- [10] Wang Hongyang,Lu Yongjun,Yao Shiming,et al.Bank and point bar morphodynamics in the Lower Jingjiang Reach of the Yangtze River in response to the Three Gorges Project[J]. *Journal of Geographical Sciences*,2022,32(8):1530–1556.
- [11] Xu Quanxi,Dong Bingjiang, Yuan Jing, et al. Scouring effect of the middle and lower reaches of the Yangtze River and its impact after the impoundment of the Three Gorges Project[J]. *Journal of Lake Sciences*,2023,35(2):650–661.[许全喜,董炳江,袁晶,等.三峡工程运用后长江中下游河道冲刷特征及其影响[J].湖泊科学,2023,35(2):650–661.]
- [12] Li Wenquan.On the effects of the channel change and regulation of channel that dredging sand at the middle and lower section of the Yangtze River[D].Wuhan:Wuhan University,2004.[李文全.长江中下游采砂对航道演变及整治工程影响研究[D].武汉:武汉大学,2004.]
- [13] Yang Yunping,Li Ming,Liu Wanli,et al.Study on the relationship between beach trough evolution and navigation obstruction characteristics in Jingjiang reach of the Yangtze River[J]. *Advances in Water Science*,2022,33(2):240–252.[杨云平,李明,刘万利,等.长江荆江河段滩槽演变与航道水深资源提升关系[J].水科学进展,2022,33(2):240–252.]
- [14] Yang Yunping,Zheng Jinhai,Zhang Mingjin,et al.Sandy riverbed shoal under anthropogenic activities: The sandy reach of the Yangtze River,China[J]. *Journal of Hydrology*,2021,603(PA):12861–12867.
- [15] Mao Ye,Huang Caian.Experimental study on effect of sand mining on riverbed deformation[J]. *Journal of Hydraulic Engineering*,2004(5):64–69.[毛野,黄才安.采砂对河床变形影响的试验研究[J].水利学报,2004(5):64–69.]
- [16] Hu Peng,Deng Shaoyi,Zhao Zixiong,et al.Hydro-sediment-morphodynamic modeling of riverbed evolution and calculation of dredging volum[J]. *Journal of Zhejiang University(Engineering Science)*,2021,55(4):733–741.[胡鹏,邓苟怡,赵自雄,等.基于水沙床耦合的滩槽冲淤模拟与疏浚量计算[J].浙江大学学报(工学版),2021,55(4):733–741.]
- [17] Luan Hualong,Yao Shiming,Qu Geng,et al.Morphological evolution of the channel-shoal system in the South Channel of the Changjiang Estuary during 1958–2018: Causes and future trends[J]. *Journal of Geographical Sciences*,2022,32(11):2291–2310.
- [18] Luan Hualong,Liu Tonghuan,Ding Pingxing.Recent morphological evolution processes and prediction on future evolution trend of the Changjiang estuary[J]. *Advanced Engineering Sciences*,2019,51(2):21–27.[栾华龙,刘同宦,丁平兴.长江口河段近期冲淤演变过程及未来趋势预测[J].工程科学与技术,2019,51(2):21–27.]
- [19] Qiao Fei,Meng Wei,Zhang Wanshun,et al.Study on the effect of sand excavation on the local riverbed variation in the Dongjiang River[J]. *Journal of Sediment Research*,2010(2):64–69.[乔飞,孟伟,张万顺,等.人工采砂对东江干流局部河段河床冲淤的影响研究[J].泥沙研究,2010(2):64–69.]
- [20] Hassen N A,Zulfequar A.Flow and morphological characteristics in mining pits of a river through numerical and experimental modeling[J]. *Modeling Earth Systems and Environment*,2022,9(1):677–692.
- [21] Yu Heli,Xia Ye,Wang Zhihan,et al.Numerical simulation study on effect of different longitudinal profile dimensions of sandpit on riverbed evolution of pebble channel—A case of Shuangsheng Section of Shiting River[J]. *Advanced Engineering Sciences*,2017,49(Supp2):83–91.[于合理,夏叶,王之晗,等.采砂坑纵剖面尺寸对卵石河道河床演变影响数值试验——以石亭江双盛段为例[J].工程科学与技术,2017,49(增刊2):83–91.]
- [22] Tran K T,Mai T N H,Quoc D N H,et al.Assessment of the impact of sand mining on bottom morphology in the Mekong River in an Giang Province,Vietnam,using a hydro-morphological model with GPU computing[J]. *Water*,2020,12(10):w12102912.
- [23] Yang Xingju,Hei Pengfei.Effect of artificial sand excavation on fluvial process of Huaihe River Bengbu to Fushan reach[J]. *Journal of Hydroelectric Engineering*,2011,19(Supp1):78–84.[杨兴菊,黑鹏飞.人工采砂对蚌浮段河床演变的影响分析[J].应用基础与工程科学学报,2011,19(增刊1):78–84.]
- [24] Jiang Ling,Li Yitian,Sun Zhaohua,et al.Channel evolution of Jingjiang Reach and its influences on waterway after impoundment of the Three Gorges Project[J]. *Journal of Hydroelectric Engineering*,2010,18(1):1–10.[江凌,李义天,孙昭华,等.三峡工程蓄水后荆江沙质河段河床演变及对航道的影 响[J].应用基础与工程科学学报,2010,18(1):1–10.]
- [25] Xia Junqiang,Lin Fenfen,Zhou Meirong,et al.Recent morphodynamic evolution of the Jiepai Reach and its effect on the navigation condition[J]. *Journal of Basic Science and*

Engineering, 2020, 28(1): 27–39. [夏军强, 林芬芬, 周美蓉, 等. 近期界牌河段河床调整及其对航道条件的影响[J]. 应用基础与工程科学学报, 2020, 28(1): 27–39.]

[26] Xu Quanxi, Li Sixuan, Yuan Jing, et al. Analysis of equilibrium sediment transport in the middle and lower reaches of the Yangtze River after the impoundment of the Three Gorges Reservoir[J]. Journal of Lake Sciences, 2021, 33(3): 806–818. [许全喜, 李思璇, 袁晶, 等. 三峡水库蓄水运用以

来长江中下游沙量平衡分析[J]. 湖泊科学, 2021, 33(3): 806–818.]

[27] Zhao Weiyang, Yang Yunping, Zhang Huaqing, et al. Adjustment patterns and causes of the morphology of sandy riverbed downstream of the Three Gorges Dam[J]. Advances in Water Science, 2020, 31(6): 862–874. [赵维阳, 杨云平, 张华庆, 等. 三峡大坝下游近坝段沙质河床形态调整及洲滩联动演变关系[J]. 水科学进展, 2020, 31(6): 862–874.]

Analysis of the Impact of Sand Mining on Erosion and Sedimentation of Sandy River Section Downstream of the Three Gorges Dam

CHEN Bingjun, XIAO Yi

(National Inland Waterway Regulation Engineering Research Center, Chongqing Jiaotong University, Chongqing 400074, China)

Abstract:

Objective The joint operation of cascade reservoirs with the Three Gorges Project as the core has changed the water and sediment conditions downstream of the dam, causing long-term and long-distance erosion and sedimentation adjustments, especially significant adjustments to the sandy riverbed near the dam section. The rapid economic development of the Yangtze River region has strengthened the demand for river sand resources in the Yangtze River Basin. Due to the dramatic sand mining activities in the downstream of the Three Gorges Dam, serious changes in the river bed level occurred, as well as beach adjustment became more complex. Since the Three Gorges Reservoir impoundment operation, the Sanday River section downstream of the Three Gorges Dam has generally shown a scouring trend, with significant changes in the pattern of beach troughs and continental shoals, and the main stream of the branch channel oscillating more, in the process of a strong adjustment of riverbed. To explore the impact of sand mining on the sediment transport process in the sandy river section, this study selected the Shashi River section as an example and constructed a two-dimensional (2D) water and sediment transport numerical model based on Delft3D.

Methods The model adopts an orthogonal adherent curve grid, the number of grids is 156×27 , the grid length in the river direction is 60–100 m, the grid length in the river width direction is 20–40 m, and the grid is interpolated by using the measured topographic data of August 2018, and the inlet and outlet boundary conditions are based on the observed flow discharge and sediment concentration data of Shashi Hydrological Station from 2019 to 2021. The median sediment size is $250 \mu\text{m}$, the initial river bed active layer thickness is 10 m, and the sediment module uses a non-equilibrium sediment transport mode with a calculation time step of 24 s. Verification of the variations in water level and sedimentation was carried out, the maximum water level difference between calculated and measured data is 0.08 m, and the water level simulation accuracy value of RMSE is 0.92, and the simulated scouring and sedimentation pattern was similar to the pattern for the measured distribution, the maximum scour depth in the main channel is about 6 m, and the amplitude of scour and deposition is 3–5 m, the measured scouring volume of the river section is $35.13 \text{ million m}^3$ while the simulated volume of $39.45 \text{ million m}^3$ with the relative error of 12%. The simulated river bed level changes of typical cross-sections agree well with the measured topographic change trend except for some areas disturbed by the human activities. The simulation results indicate that the developed 2D numerical model has the capable of investigating the influence of sand mining on the river pattern changes in the Shashi River Section. Next, the generalized sand mining pits were set in the Shashi River section based on the investigation of the sand mining activities, and simulated and analyzed the changes in erosion-deposition pattern and sediment concentration distribution with and without sand mining.

Results and Discussions The analysis results indicate that small-scale river sand mining has a relatively tiny effect on the sediment transport process in the Shashi River section. The influence range of sediment concentration is within 1 km upstream and downstream of the sand mining pit, and the variation in the sediment concentration during the dry season is $0.004\text{--}0.006 \text{ kg/m}^3$. During the flood season, a significant change occurs primarily in the area of sand mining pits, with the maximum variation being 0.016 kg/m^3 . However, the erosion and deposition characteristics of the river section remain unchanged, with the main erosion and deposition distribution being comparable under both sand mining and non-sand mining conditions. The sand mining pit has a slight effect on the sediment scouring and siltation pattern in the upstream and downstream of the pit within a range of about 1 km, and the changes in the river bed level were $-0.1\text{--}0.1 \text{ m}$. The sediment behavior triggered by the increase of near-bottom flow velocity in the upstream of the sandpit resulted in a tiny increase in erosion. Nevertheless, the Shashi River section under sand min-

ing conditions has witnessed a 2.25 million m^3 reduction in erosion amount compared to the condition without sand mining. The amount of erosion and sedimentation in the Shashi River section varies by 6% with and without sand mining. The self-recovery capabilities of the sand excavation pits are closely related to the local incoming water and sediment discharge. Both 2019 and 2021 were normal hydrological years with sediment discharges of approximately 18.8 million tons, whereas 2020 was a year of high water and sediment discharge, resulting in a sediment discharge of 58.7 million tons. The averaged annual deposition rate of the borrow pits is 10%~25%, with a deposition depth of 0.9~1.3 meters and a recovery period of about 4~10 years. However, in abnormal hydrological years (such as high water and sediment discharge), the recovery deposition volume increased to 600 thousand m^3 , the maximum sedimentation depth reached 7 m, and the mean annual sedimentation rate can attain to 50%. In years of high water and sediment discharge, the recovery period of sand pits is shortened.

Conclusions This paper explores the impact of small-scale sand mining activities on the erosion and deposition characteristics in the typically sandy river section downstream of the Three Gorge Dam, utilizing the developed two-dimensional (2D) water and sediment transport numerical model. The conclusions of this study provide more accurate and reliable foundational conditions for studying sediment issues in the downstream of the Three Gorges Dam, conducting numerical simulations, creating physical models, and offer substantial support for the scientific management of sand mining in the planning stages along the Yangtze River Basin.

Key words: Shashi River section; sand mining; erosion and sedimentation; recovery capacity of sand pits; downstream of the Three Gorges Dam

(编辑 张 琼)

引用格式:Chen Bingjun,Xiao Yi.Analysis of the impact of sand mining on erosion and sedimentation of sandy river section downstream of the Three Gorges Dam[J].Advanced Engineering Sciences,2025,57(3):201-209.[陈柄君,肖毅.采砂活动对三峡坝下游沙质河段泥沙冲淤影响研究[J].工程科学与技术,2025,57(3):201-209.]